



Effect of laser energy on optical properties of lead sulfide nanostructures

M. Sadeldine

Laboratoire de Physique et Mécanique des Matériaux, Sultan Moulay Slimane Université, Béni-Mellal, Morocco

Email: msadeldine@usms.ma

Received 1/10/2024, Received in revised form 28/11/2024, Accepted 9/12/2024, Published 15/1/2025

This study investigates the influence of laser energy on the optical properties of lead sulfide (PbS) nanostructures deposited using the pulsed laser deposition (PLD) technique. Thin films were synthesized on glass substrates at room temperature using an Nd:YAG laser with varying energy levels (200, 300, 400, and 500 mJ). Structural analysis through X-ray diffraction (XRD) confirmed a polycrystalline cubic phase, while atomic force microscopy (AFM) revealed an increase in grain size with higher laser energy. Optical characterization showed that absorbance increases with laser energy, while transmittance decreases due to enhanced scattering and larger grain sizes. The absorption coefficient varied between $9 \times 10^4 \text{ cm}^{-1}$ and $42 \times 10^4 \text{ cm}^{-1}$, confirming direct allowed transitions. The optical bandgap ranged from 1.8 eV to 1.25 eV, decreasing with increasing laser energy, indicating changes in particle size and density. Furthermore, variations in the refractive index, extinction coefficient, and dielectric constants were analyzed, demonstrating a significant dependence on laser energy. These findings highlight the potential of tuning PbS thin film properties for applications in optoelectronics and photovoltaic devices.

Keywords: Lead sulfide; Nanostructure; Optical.

1. INTRODUCTION

Lead sulfide (PbS) is a semiconductor material with remarkable optical and electronic properties, making it highly suitable for applications in photodetectors, photovoltaics, and optoelectronic devices. Due to its narrow direct bandgap and high absorption coefficient, PbS is extensively utilized in infrared (IR) sensors, solar cells, and quantum dot-based technologies. The optical and structural properties of PbS thin films are strongly influenced by the deposition technique and processing parameters, particularly laser energy in pulsed laser deposition (PLD) [1-3].

Pulsed laser deposition (PLD) is a versatile and efficient technique for fabricating high-quality thin films. By controlling laser parameters such as energy, pulse duration, and repetition rate, it is possible to

manipulate the structural and optical characteristics of the deposited films. The interaction between the laser beam and the target material determines the film's crystallinity, grain size, and surface morphology, which in turn affect its optical behavior. Previous studies have shown that higher laser energy leads to increased surface roughness, larger grain sizes, and enhanced light absorption, impacting key optical parameters such as transmittance, refractive index, and bandgap energy [4-6].

In this study, PbS nanostructured thin films were deposited on glass substrates using an Nd:YAG laser with varying energy levels to investigate the effect of laser energy on their optical properties. The films were characterized using X-ray diffraction (XRD) to analyze crystallinity, atomic force microscopy (AFM) to study surface morphology, and ultraviolet-visible (UV-Vis) spectroscopy to evaluate optical absorption and transmittance. By understanding how laser energy influences these properties, this research aims to optimize PbS thin films for enhanced performance in optoelectronic and photovoltaic applications [7-9].

2. EXPERIMENTAL

The pulsed laser deposition (PLD) system, housed in the Plasma Research Laboratory of the Physics Department at the College of Science, University of Baghdad, was utilized for this experiment. The deposition process was carried out in a vacuum chamber under a pressure of 2.5×10^{-2} mbar. The PbS target was prepared by applying a pressure of 6 tons for 10 minutes using a SPECAC hydraulic piston, forming a disc with a diameter of 1.5 cm and a thickness of 0.3 cm. Glass slides were used as substrates to analyze the surface composition and morphological properties of the PbS films.

The experimental setup involved precise positioning of the substrate holders and target inside the chamber relative to the laser beam. An Nd:YAG laser with a wavelength of 1064 nm, pulse energies of 200, 300, 400, and 500 mJ, a frequency of 6 Hz, and a total of 100 laser pulses was used for deposition. The Nd:YAG SHG Q-switched laser beam entered the chamber through a window at an angle of approximately 45 degrees to the target surface. The PLD system consists of two vacuum systems: a two-stage rotating vacuum system and a diffusion vacuum system. Additionally, the system is equipped with pressure and temperature gauges, as well as a vacuum chamber.

The deposited thin films were analyzed using various characterization techniques. X-ray diffraction (XRD) was employed to examine the crystal structure, while atomic force microscopy (AFM) was used to study surface morphology. Furthermore, ultraviolet (UV) spectroscopy was performed to evaluate the optical properties of the PbS films.

3. RESULTS AND DISCUSSION

The structural characteristics of PbS thin films were examined using X-ray diffraction (XRD) and atomic force microscopy (AFM). The XRD patterns confirmed that all deposited films exhibited a polycrystalline cubic structure, with dominant diffraction peaks corresponding to the (111) and (200) planes. The crystallite size was calculated using the Scherrer equation, revealing an increase in grain size with higher laser energy. At 200 mJ, the smallest crystallite size recorded was 59.43 nm, while at 500 mJ, the crystallite size increased due to enhanced kinetic energy of the ablated particles, promoting crystal growth (Figure 1) [10-12].

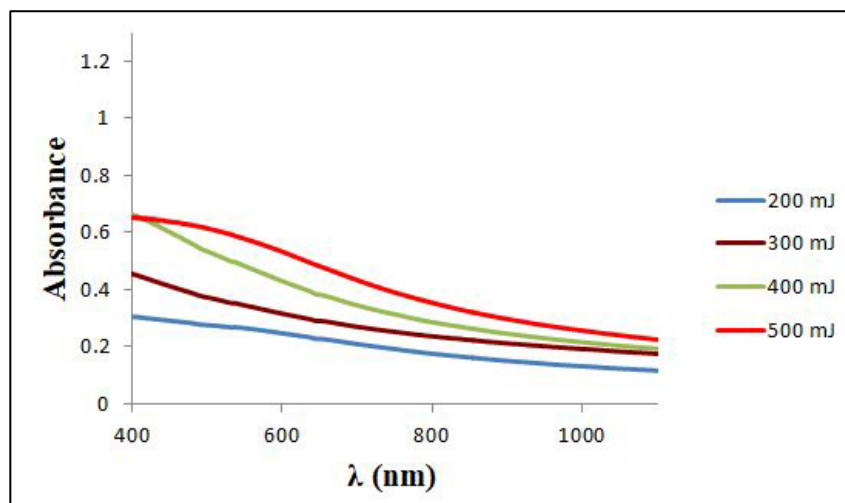


Figure 1 Absorbance as a function of wavelength of PbS films deposited at different laser energies.

Atomic force microscopy (AFM) images provided further insight into the surface morphology of the PbS films. The root mean square (RMS) roughness increased with laser energy, indicating that higher energy promotes the formation of larger grains and a rougher surface. This roughness enhancement is attributed to the higher mobility of adatoms on the substrate surface, which facilitates grain coalescence [13-15]. As a result, films deposited at higher laser energies exhibited a more pronounced grain structure, impacting their optical behavior (Figure 2).

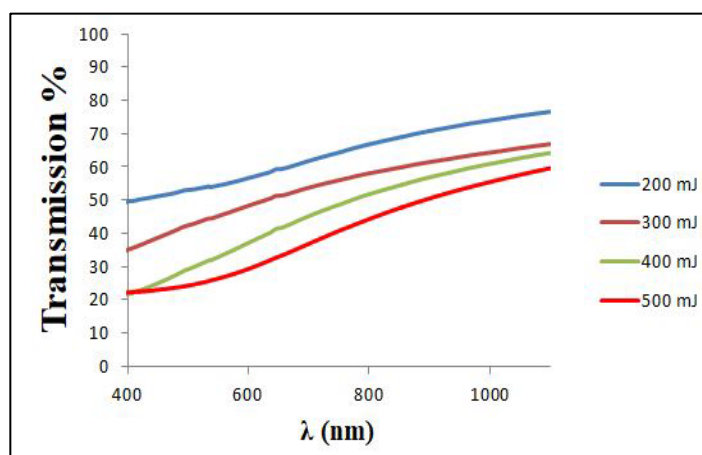


Figure 2 Transmittance as a function of wavelength of PbS membranes deposited at different laser energies.

The optical properties of the PbS thin films were studied using UV-Vis spectroscopy, focusing on absorbance, transmittance, and the optical bandgap. The absorption spectrum, shown in Figure 1, revealed that the absorbance of PbS films increased with higher laser pulse energy. This increase in absorption can be attributed to the enhanced grain size and surface roughness, which result in greater photon trapping. The highest absorbance was observed for films deposited at 500 mJ, with the primary absorption edge positioned in the UV region [16-18]. As the wavelength increased, absorbance

decreased, extending into the visible spectrum, consistent with the material's bandgap characteristics (Figure 3).

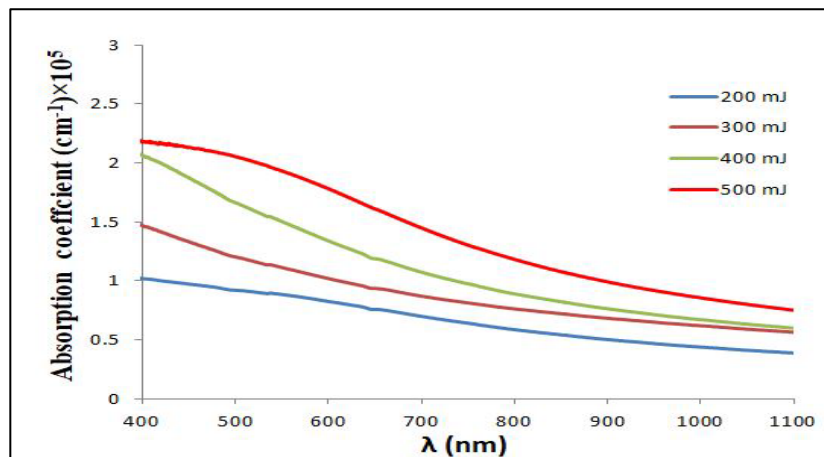


Figure 3 Absorption coefficient α as a function of wavelength of PbS films deposited at different laser energies.

The transmittance spectra, presented in Figure 2, demonstrated that transmittance decreases as laser energy increases. Films deposited at 200 mJ exhibited the highest transmittance of 76.5% in the infrared (IR) region, while those deposited at 500 mJ showed reduced transmittance due to increased surface roughness and scattering effects. The inverse relationship between transmittance and laser energy is attributed to the formation of larger grain sizes and surface irregularities that enhance light absorption rather than transmission [19-22]. The absorption coefficient (α) was calculated using the relation:

$$A = \log\left(\frac{1}{T}\right) \quad (1)$$

where A is the absorbance, and t is the film thickness. As shown in Figure 3, the absorption coefficient increased with laser energy, ranging from $9 \times 10^4 \text{ cm}^{-1}$ to $42 \times 10^4 \text{ cm}^{-1}$. This trend suggests that higher laser energy leads to increased optical absorption due to improved crystallinity and enhanced grain size. The high absorption coefficient ($>10^4 \text{ cm}^{-1}$) confirms that the PbS films exhibit direct electronic transitions, making them suitable for optoelectronic applications (Figure 4).

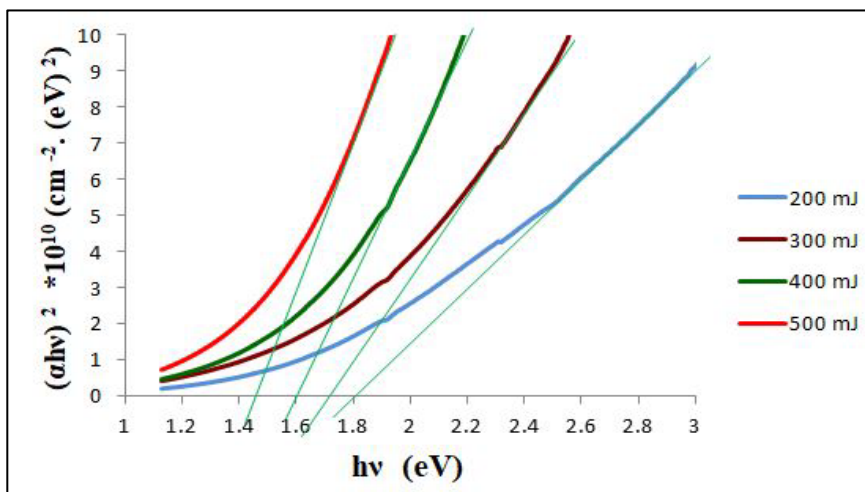


Figure 4 Demonstrates the relationship of $(\alpha h\nu)^2$ as a function of the photon energy of the prepared PbS films by changing the laser energy.

The optical bandgap energy (E_g) was determined using Tauc’s relation:

$$\alpha = \frac{(2.303 \times A)}{t} \tag{2}$$

where $h\nu$ is the photon energy, A is a constant, and n is 2 for direct bandgap materials. The extrapolated values from the Tauc plot (Figure 4) indicated that the bandgap decreases from 1.8 eV at 200 mJ to 1.25 eV at 500 mJ. This reduction in bandgap energy with increasing laser energy is associated with quantum confinement effects and increased grain size. Larger grains reduce the density of grain boundaries, minimizing defects that contribute to energy level broadening, leading to a decrease in the optical bandgap.

The refractive index (n) was calculated using the equation:

$$(\alpha h\nu) = A(h\nu - E_g)^r \tag{3}$$

where R is the reflectance. The refractive index, shown in Figure 5, decreases with increasing laser energy but exhibits a gradual increase at longer wavelengths. The highest refractive index was observed for films deposited at 200 mJ, consistent with the findings in previous literature. The extinction coefficient (k), representing energy dissipation within the material, increased with laser energy, as depicted in Figure 6. This trend suggests enhanced light absorption and internal scattering, further supporting the influence of laser energy on film optical behavior (Figure 5).

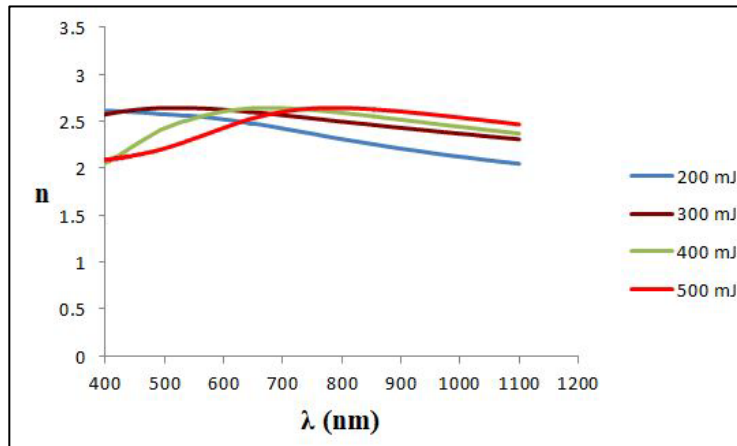


Figure 5 Refractive index (n) as a function of the wavelength of PbS films deposited at different laser energies

The dielectric constant, divided into its real (ϵ_r) and imaginary (ϵ_i) components, was analysed to understand the electronic response of PbS films. The real dielectric constant, calculated as:

$$n = \left[\left(\frac{1+R}{1-R} \right)^2 - (k^2 + 1) \right]^{1/2} + \frac{1+R}{1-R} \tag{4}$$

decreased with increasing laser energy due to the reduction in refractive index values. In contrast, the imaginary dielectric constant, given by:

$$\epsilon_1 = n^2 - k^2 \tag{5}$$

$$\epsilon_2 = 2nk \tag{6}$$

an increasing with laser energy, as shown in Figures 7 and 8. This increase is primarily influenced by the extinction coefficient, which reflects greater light absorption at higher energy levels. These variations highlight the strong dependence of PbS film optical behaviour on laser energy, making it a key factor in optimizing material properties for specific applications (Figure 6).

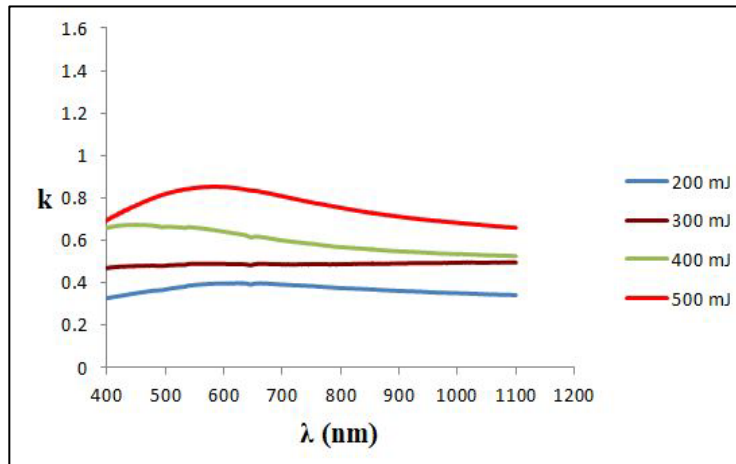


Figure 6 Extinction Coefficient (k) as a function of wavelength of PbS films deposited at different laser energies.

The results of this study demonstrate that laser energy significantly influences the structural and optical properties of PbS thin films. Higher laser energy enhances crystallinity, increases grain size, and promotes stronger light absorption, leading to a decrease in the optical bandgap. The observed trends align with previous research on laser-deposited semiconductor films, confirming that controlling laser energy allows for precise tuning of PbS film properties (Figures 7 & 8).

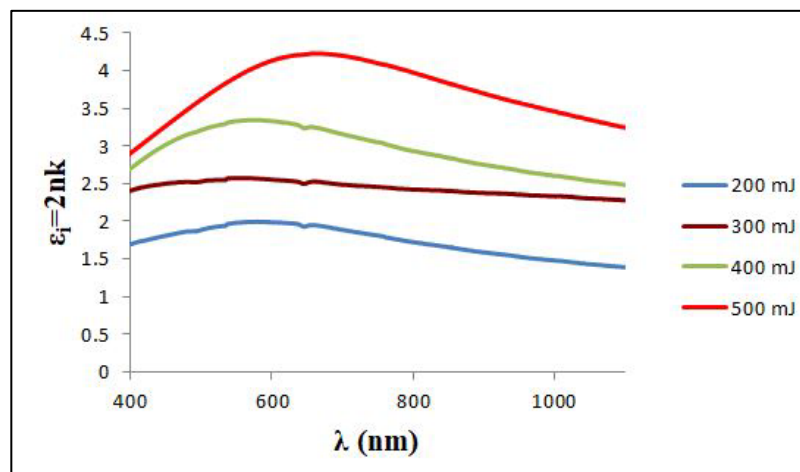


Figure 7 The Variation of The Dielectric Constants real part (ϵ_r) With Wavelength of PbS Films with Different laser energies.

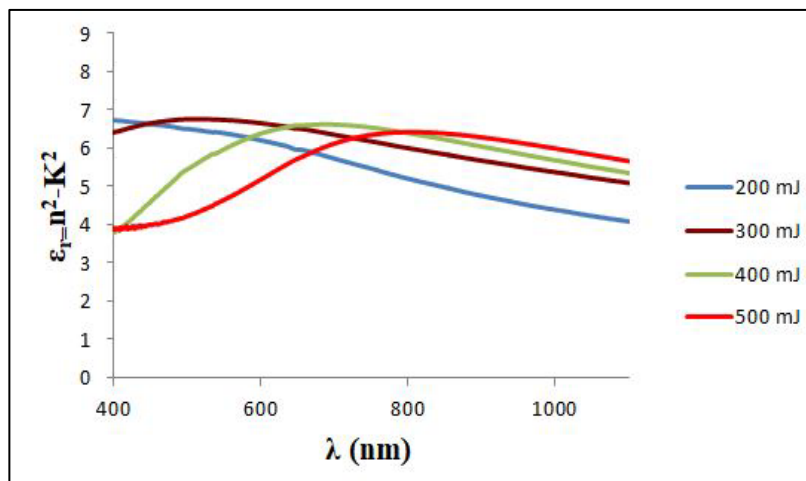


Figure 8 The Variation of The Dielectric Constants imaginary (ϵ_i) parts With Wavelength of PbS Films with Different laser energies.

From an application perspective, PbS films with lower bandgaps and higher absorption coefficients are highly desirable for infrared detectors and solar cells. The ability to manipulate these properties via PLD parameters provides an efficient approach to optimizing PbS films for optoelectronic applications. Further studies could explore post-deposition annealing and doping effects to further refine PbS film characteristics (Table 1).

Table 1 Demonstrates the change of optical parameters with the change in laser power at wavelength $\lambda = 500$ nm.

E (mJ)	T%	α (cm ⁻¹)	K	n	ϵ_r	ϵ_i	Eg (eV)
200	53.06	91899	0.366	2.676	6.702	1.885	1.80
300	42.36	120263	0.479	2.643	6.557	2.531	1.72
400	29.20	166193	0.662	2.428	5.455	3.212	1.60
500	24.27	205312	0.817	2.213	4.228	3.617	1.47

4. CONCLUSIONS

This study highlights the significant impact of laser energy on the optical properties of PbS nanostructured thin films. The results confirm that increasing laser energy enhances crystallinity, increases grain size, and shifts the optical bandgap. Optical measurements demonstrated strong absorption in the UV region, reduced transmittance with higher laser energy, and variations in refractive index and dielectric properties. These findings provide valuable insights into optimizing PbS films for advanced optoelectronic and photovoltaic applications.

References

[1] G. Le Marie, C. Cière, C. Selvain, Exp. Theo. NANOTECHNOLOGY 5 (2021) 1
 [2] M. N. Ashfold, F. Claeysens, G. M. Fuge, and S. J. Henley, Chemical Society Reviews 33 (2004) 31

- [3] C. O. Mosiori, W. Njororge, and J. Okumu, *International Journal of Advanced Research in Physical Science* 1 (2014) 32
- [4] M. Gunasekaran and M. Ichimura, *Japanese Journal of Applied Physics* 44 (2005) 7345
- [5] S. M. Lee and Y. S. Cho, *Journal of Alloys and Compounds* 579 (2013) 283
- [6] L. Yu, Y. Lv, G. Chen, X. Zhang, Y. Zeng, H. Huang, *Inorganica Chimica Acta* 376 (2011) 663
- [7] S. Seghaier, N. Kamoun, R. Brini, and A. Amara, *Materials Chemistry and Physics* 97 (2006) 80
- [8] Y. Z. Dawood, S. M. Kadhim, and A. Z. Mohammed, *Engineering and Technology Journal* 33 (2015) 1730
- [9] X. Feng, H. Dao, W. Zhang, *Exp. Theo. NANOTECHNOLOGY* 5 (2021) 7
- [10] G. A. Al-Dahash, T. A. Al-Abas, and W. A. Al Dayem, *Australian Journal of Basic and Applied Sciences* 9 (2015)139
- [11] M. Hermann, F. Bansil, H.A. Hunter, *Exp. Theo. NANOTECHNOLOGY* 5 (2021) 13
- [12] M. Al-Kinany, G. A. Al-Dahash, and J. Al-Shahban, *Australian Journal of Basic and Applied Sciences* 8 (2014) 289
- [13] T. Asanuma, T. Matsutani, C. Liu, T. Mihara, and M. Kiuchi, *Journal of Applied Physics* 95 (2004) 6016
- [14] M. Al-Kinany, G. A. Al-Dahash, and J. Al-Shahban, *Engineering and Technology Journal* 33 (2015) 1570
- [15] J. Yang, M. V. Reddy, *Exp. Theo. NANOTECHNOLOGY* 5 (2021) 23
- [16] Badis Bendjemil, Maram Mechi, Khaoula Safi, Mounir Ferhi, Karima Horchani Naifer, *Exp. Theo. NANOTECHNOLOGY* 8 (2024) 51
- [17] K. AADIM, A. IBRAHIM, and J. MARIE, *International Journal of Physics* 5 (2017) 8
- [18] A. M. Ahmed Alwaise, Raqeeb H. Rajab, Adel A. Mahmood, Mohammed A. Alreshedi, *Exp. Theo. NANOTECHNOLOGY* 8 (2024) 67
- [19] K. Sundaram and G. Bhagavat, *Journal of Physics D: Applied Physics* 14 (1981) 921
- [20] A. Bendavid, P. Martin, and L. Wiczorek, *Thin Solid Films* 354 (1999) 175
- [21] M. Abbas, A. A.-M. Shehab, A. Al-Samuraee, and N. Hassan, *Energy Procedia* 6 (2011) 250
- [22] J. Román-Zamorano, M. Flores-Acosta, H. Arizpe-Chávez, F. Castellón-Barraza, M. Farías, and R. Ramírez-Bon, *Journal of Materials Science* 44 (2009) 4788

